Field-driven geometrical phases in a time-periodic quantum system

P. Brusheim*
Division of Solid State Physics, Lund University, Box 118, S-22100 Lund, Sweden
and Institute of High Performance Computing, 1 Fusionopolis Way, #16-16 Connexis, Singapore 138632, Singapore

H. Q. Xu†
Division of Solid State Physics, Lund University, Box 118, S-22100 Lund, Sweden
(Received 31 March 2009; revised manuscript received 30 April 2009; published 29 May 2009)

We apply Floquet theory to explore the geometry of the Hilbert space under the influence of a time-periodic field. The geometrical phase is found to be induced by field-driven hybridizations when the photon energy of the driving field is close to the transition energies of the states of a quantum system. The phases of two hybridized states are phase locked to each other. We show that the geometrical phase is in general related to the Rabi frequency of the hybrid states. We also show that when the photon energy is equal to the transition energy of two states the geometrical phase acquired by each state is given exactly by an integer multiple of π, independent of the strength of the driving field. We illustrate the derived generic properties of the geometric phase with an experimentally realizable quantum-wire system. It is shown that the interference between conductance channels in the wire presents a way to identify the geometrical phase.

DOI: 10.1103/PhysRevB.79.205323 PACS number(s): 73.21.La, 73.21.Hb, 03.65.Vf

I. INTRODUCTION

The phase of the wave function lies at the heart of the quantum-mechanical description of reality. In a seminal work, Berry[1] derived that a quantum system evolving adiabatically around a closed path (circuit) in parameter space acquires, apart from the expected dynamical phase, a geometrical phase which is related to the curvature of the traced-out circuit in parameter space.[2] Aharonov and Anandan generalized this important result to nonadiabatic evolutions[3] and showed that the geometrical phase is a nonlocal property.[4] They furthermore showed that the system does not necessarily have to undergo a cyclic evolution through a circuit in parameter space but rather the geometrical phase arises due to the evolution of the states themselves around a circuit in the projective Hilbert space defined by the map $\Pi(\psi)=\{\psi':\psi'=c\psi, c\in\mathbb{C}\}$, i.e., a closed path in the space spanned by the eigenvectors differing by more than a scaling and/or a phase factor. The phase is then a direct consequence of the holonomy, namely, the curvature, of the circuit in the projective Hilbert space.[5,6] An eigenstate of a quantum system subjected to a time-periodic electromagnetic field is undergoing such a cyclic evolution and would be expected to absorb information on the projective space topology. The geometrical phase, and its adiabatic-limit Berry phase, thus impose far reaching implications in various fields of physics and is currently being studied in regard to, e.g., the quantum-Hall effect in graphene,[7,8] superconducting charge pumps,[9] semiconductor heterostructures,[10,11] and quantum information.[12,13]

In this paper, we employ the Floquet theory to explore the geometrical phase of the Hilbert space under the influence of a time-periodic field. We show that by driving the system into a level hybridization a nontrivial geometrical phase related to the Rabi frequency of the transition emerges. We also examine time-periodic field-driven low-dimensional quantum systems and illustrate the derived generic properties of the geometric phase with these experimentally realizable dynamic quantum systems.

II. FORMALISM

A. Quasienergy spectrum and the geometric phase

The Floquet theory presents an elegant formalism for calculating cyclic states, energy spectra, and geometrical phases of a time-periodic quantum system.[14–16] We here give a brief introduction to this formalism. Let us start with considering a time-periodic quantum system evolving at frequency ω such that its Hamiltonian satisfies $H(t+\tau)=H(t)$ for a period $\tau=2\pi/\omega$. The solutions $\psi(t)$ to the Schrödinger equation of the system will define a path $C:t\rightarrow t+\tau$, not necessarily closed, in Hilbert space. This path describes a circuit in the projective Hilbert space since $\psi(t+\tau)=e^{i\phi}\psi(t)$. The Floquet theorem guarantees a solution to the time-dependent Schrödinger equation with the Hamiltonian $H(t)$ on the form $\Psi_\alpha=e^{-i\varepsilon_\alpha t}\Phi_\alpha(t,\sigma,\mathbf{r})$, where the Floquet modes Φ_α, besides being functions of spin σ and position $\boldsymbol{r}$, are time periodic with period τ. Here we note that we adopt the atomic units in the formalism by setting $\hbar=m_e=e=1$ throughout the paper. The quasienergies ε_α for the time-periodic quantum system are defined in analogy to the quasimomenta of the Bloch states in a spatially periodic system.[16] The Schrödinger equation now reduces to

$$\mathcal{H}\Phi_\alpha=\varepsilon_\alpha\Phi_\alpha, \tag{1}$$

with $\mathcal{H}=H-i\partial/\partial t$, which is structurally equivalent to a time-independent eigenvalue equation and implies that we can formally apply all theorems characteristic for time-independent Schrödinger theory to the periodically driven quantum system. In particular, by applying the Hellman-Feynman theorem it can be shown that the geometrical phase of a Floquet state Ψ_α in the time-periodic system takes the form[16] $\chi_\alpha=-2\pi\frac{\partial\varepsilon_\alpha}{\partial\omega}$. This equation is of a remarkably simple form and implies that all the information of the time-periodic field-induced geometrical phase (and hence information on the projective Hilbert-space topology) is contained in the quasienergy spectrum.

Let V_{ac} be the strength of the perturbing time-periodic field. For an adiabatic switch off of the field the quasienergies satisfy[16]

$$\lim_{V_{\mathrm{ac}}\to 0} \varepsilon_\alpha = \varepsilon_\alpha^0 = E_q^0 + n\omega, \quad n \in \mathbb{Z}, \tag{2}$$

with the associated eigenstates

$$\lim_{V_{\mathrm{ac}}\to 0} \Psi_\alpha = \Psi_\alpha^0 = e^{in\omega t}\Phi_q^0(\sigma,\mathbf{r}), \tag{3}$$

where E_q^0 and $\Phi_q^0(\sigma,\mathbf{r})$ are solutions to the time-independent part of the Hamiltonian. Equations (2) and (3) define the unperturbed eigenstates dressed by integer number of absorbed or emitted photons. The eigenstates in this limit are naturally stationary states in the projective Hilbert space. They thus describe a vanishing circuit and the geometrical phase consequentially takes the trivial values of $\chi_\alpha^0 = 0 + 2\pi m$, $m \in \mathbb{Z}$.

B. Phase evolution in a two-level system

Due to the linear dependence on frequency in Eq. (2), it can occur that a pair of dressed unperturbed levels crosses at some frequency $\omega_0 = (E_q^0 - E_{q'}^0)/(n'-n)$. For a nonzero field amplitude, $V_{\mathrm{ac}} > 0$, the solutions of the two-level system close to the crossing point take the mixture state form $\Psi(t) = e^{-i\varepsilon t}[c_\alpha(t)\Psi_\alpha^0(t) + c_{\alpha'}(t)\Psi_{\alpha'}^0(t)]$ and the quasienergy levels show anticrossings.[17] The cyclic evolution of each mixture state defines a finite circuit in the projective space spanned by $\{\Psi_\alpha^0, \Psi_{\alpha'}^0\}$ and the geometrical phase is related to the hybridization of the stationary eigenstates. Close to a crossing point of two unperturbed quasienergy levels ε_α^0 and $\varepsilon_{\alpha'}^0$, the quasienergy levels can be written as

$$\varepsilon = \bar{E} \pm \sqrt{\left(\frac{\Delta E}{2}\right)^2 + |V|^2}, \tag{4}$$

where V is the off-diagonal matrix element due to the driving field, $\bar{E} = (E_q^0 + E_{q'}^0)/2 + (n+n')\omega/2$ is the mean value of the levels in the absence of the mixing, and $\Delta E = (\omega - \omega_0)(n - n')$ is their difference. The corresponding eigenvectors read $\Psi(t) = e^{-i\varepsilon t}\Phi(t)$ with

$$\Phi(t) = \frac{e^{i\beta}\gamma e^{in\omega t}\Phi_\alpha^0(\sigma,\mathbf{r}) + e^{in'\omega t}\Phi_{\alpha'}^0(\sigma,\mathbf{r})}{\sqrt{\gamma^2+1}}, \tag{5}$$

where $\gamma = [(\Delta E/2) \pm \sqrt{(\Delta E/2)^2 + |V|^2}]/|V|$ and β is defined by $V = |V|e^{i\beta}$.

Assume that the time-periodic quantum system is driven by an external monochromatic uniform field and the Hamiltonian $\mathcal{H}$ of the system with the driving field is invariant under a generalized-parity operator P with eigenvalues $p = \pm$ corresponding to even- and odd-parity states.[16] In general the parity operator takes the form $P = P_t P_r P_s$, where P_t is a time-parity operator, P_r is a spatial parity operator, and P_s is a spin-parity operator. The parity eigenvalue then decomposes into the product $p = p_t p_r p_s$ with each $p_{t,r,s} = \pm 1$. The explicit form of the parity operators which forms a conserved property depends on the particular form of the Hamiltonian. For a specific example see Sec. III A.

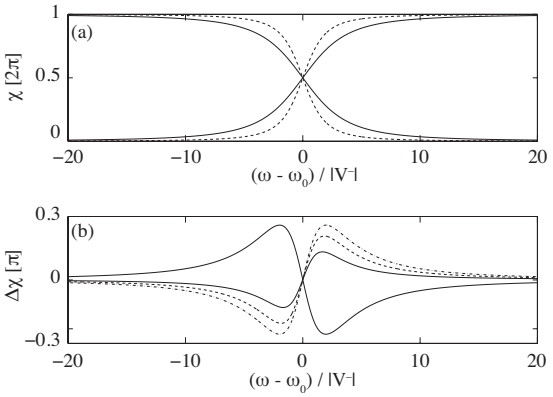

FIG. 1. (a) Geometrical-phase evolution at frequencies close to an anticrossing point calculated from Eq. (7) with $n=1$ and $n'=0$. Thick lines are from the positive branch and thin lines are from the negative branch, of Eq. (7). Dashed lines are for a state of weak interaction strength $|V^-|$ and solid lines are for a state of strong interaction strength $|V^+| = 4|V^-|$. (b) Phase difference between states of unequal interaction strengths, $|V^+| = 2|V^-|$ (thick solid line), $|V^+| = 3|V^-|$ (dashed line), and $|V^+| = 4|V^-|$ (dashed-dotted line). Thin solid line from negative branch with $|V^+| = 4|V^-|$.

The unperturbed Floquet states of the system given in Eqs. (2) and (3) can be separated into two sets according to their parities. Two states of different parities do not interact with each other while two states of the same parity show anticrossing behavior in the quasienergy spectrum in the presence of the driving field. In general, the matrix element $|V^p|$ of the driving field between two unperturbed Floquet states is parity dependent. Taking this into account, the geometrical phases of the two perturbed states given in Eqs. (4) and (5) can be found from

$$\frac{\chi^p}{2\pi} = \mp\frac{1}{2}\frac{(n'-n)^2(\omega-\omega_0)}{\sqrt{(\omega-\omega_0)^2(n'-n)^2 + 4|V^p|^2}} - \frac{n'+n}{2}, \tag{6}$$

up to the ambiguity of adding $2\pi m$. The phases of the two branches $(\pm)$ of the same parity (p) are locked with opposite sign at all frequencies since $\chi_+^p + \chi_-^p = 2\pi(n'+n) + 2\pi m$. In Sec. III B we will see how this phase locking has an interesting consequence for the measurement of the geometrical phase.

For a monochromatic linearly polarized driving field $V_{\mathrm{ac}} = V_{\mathrm{ac}}^0 \mu \cos(\omega t)$, where μ is the dipole moment operator, we obtain $|V^p|^2 = (V_{\mathrm{ac}}^0)^2|\mu^p|^2(\delta_{n',n+1} + \delta_{n',n-1})/4$. Here μ^p is the matrix element of the dipole moment operator between two unperturbed Floquet states of parity p. By identifying the Rabi frequency $\Omega_{n',n}^R = \sqrt{(\omega-\omega_0)^2(n'-n)^2 + (V_{\mathrm{ac}}^0)^2|\mu^p|^2(\delta_{n',n+1} + \delta_{n',n-1})}$, we find

$$\frac{\chi^p}{2\pi} = \mp\frac{1}{2}\frac{(n'-n)^2(\omega-\omega_0)}{\Omega_{n',n}^R} - \frac{n'+n}{2}. \tag{7}$$

Equation (7) shows [cf. Fig. 1(a)] that under the interaction with the time-periodic driving field, the Floquet states of the quantum system around an anticrossing point acquire a phase after a cyclic evolution. Away from the anticrossing point the phase tends to the trivial values expected for the case of a

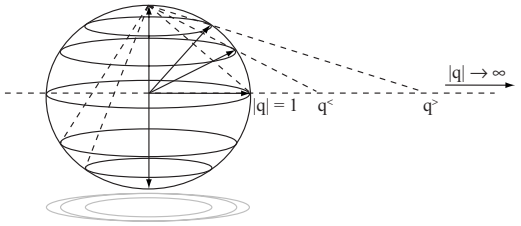

FIG. 2. Stereographic projection of the eigenstates onto the Bloch (Riemann) sphere. Away from a quasienergy anticrossing point both parity states point to a pole. Close to the quasienergy anticrossing point the parity states separate and describe different circuits on the sphere. At the anticrossing point both parity states precess around the equator and acquire the same geometrical phase.

vanishing driving field. Remarkably, the geometrical phase at the anticrossing point, where a complete hybridization is expected, is an integer multiple of π independent of the strength of the driving field. Furthermore, at this point the phases are equal for both anticrossing states of both parities. At all other points, a difference in the geometrical phase between two Floquet states of different parities can appear due to $|V^+| \neq |V^-|$ [cf. Fig. 1(b)]. For equal amplitudes of the off-diagonal matrix elements this phase difference vanishes and hence the parity degeneracy of the geometrical phase is restored This is also true in the case of $(\omega - \omega_0) \to \pm\infty$ for $|V^+| \neq |V^-|$. As is seen in Fig. 1(b) the phase difference goes through an antisymmetrical dip-peak-like structure as the frequency traverses through the degeneracy point. The dip-peak amplitude increases with increasing difference in the magnitude of the off-diagonal matrix elements, which in turn gives a larger degeneracy lifting.

We can understand these features from a geometric point of view by considering the stereographic projection of the eigenstates onto the Bloch (Riemann) sphere as shown in Fig. 2. Two pure states are represented by two unit vectors pointing to the north and the south poles of the sphere from the center. Consider the ratio $q = \gamma e^{i(n-n')\omega t + i\beta}$ of the two amplitudes in Eq. (5), which defines a point on the complex plane containing the equator of the sphere. A solution $\Psi(t) = e^{-i\varepsilon t}\Phi(t)$ with $\Phi(t)$ given in Eq. (5) is represented by a unit vector pointing from the center to the point where the sphere and the straight line which passes through the north pole and point q intersect. It is evident that this state vector is always at an angle θ to the north pole axis defined by $\theta = 2 \operatorname{arccot} \gamma$. The time evolution of the state vector traces a circuit on the sphere in a time interval of $\tau/(n-n')$ and the geometrical phase of the state developed under the interaction with the driving field in a period of τ is $\chi^p = (n-n')\eta$, up to the ambiguity of adding $2\pi m$, where $\eta = \pi(1 - \cos\theta)$ is half of the solid angle subtended by the circuit, traced by the state vector on the sphere, at the center.

For a vanishing magnitude of the mixing matrix element, γ and hence $|q|$ tend to infinity (zero), resulting in a projection onto the north (south) pole of the sphere, representing a pure stationary state $\Phi^0_\alpha(\sigma, \mathbf{r})$ $[\Phi^0_{\alpha'}(\sigma, \mathbf{r})]$. At the other extreme of an infinite magnitude of the mixing matrix element, γ tends to a positive or a negative unity and q describes the complex unit circle, i.e., the projections onto the equator of the sphere, indicating that the two Floquet states are formed by full hybridizations of the two stationary states. Now, assume that the off-diagonal element is a finite nonzero value. At the crossing point we have $\Delta E = 0$ and thus $\gamma = \pm 1$, irrespective of the actual value of V^p. The state vectors of all the four states (two for each parity) found in Eqs. (4) and (5) will then precess around the equator of the sphere. Thus $\eta = \pi$ and the geometrical phases of all the states are given by $\chi^p = (n + n')\pi + 2\pi m$. This is an appealing example of the fact that the geometrical phase is solely determined by the circuit traced by a state in a projective space, irrespective of the Hamiltonian from which the state was generated. Now, consider the two upper-branch states in the case $|V^+| > |V^-|$ [cf. the solid lines in Fig. 1(b)]. When the frequency is on the negative side of the crossing point, i.e., when $\omega < \omega_0$, one can show for $n > n'$ and thus $\Delta E < 0$ that $|q^+| > |q^-|$ and $|q^\pm| < 1$ for both parity states. Since $q^\pm$ are inside the complex unit circle, the two upper-branch states will project onto the southern hemisphere and the positive-parity state vector will trace a larger circuit on the sphere than its negative-parity counterpart. Thus the geometrical phases of the two upper-branch states are separated and satisfy $\chi^+ < \chi^-$. When going to the positive side of the crossing point, i.e., when $\omega > \omega_0$, one has $|q^+| < |q^-|$ and $|q^\pm| > 1$. Thus, $q^\pm$ lie outside the unit circle and the two upper-branch states are now projected onto the northern hemisphere. As a result, the positive-parity state vector will again trace the larger circuit on the sphere but the two geometrical phases satisfy $\chi^+ > \chi^-$. A similar discussion can be made for the two lower-branch states and for $|V^+| < |V^-|$.

III. NUMERICAL EXAMPLE: A QUANTUM WIRE

A. Quasienergy spectrum and the geometric phase

We now illustrate our generic findings by considering a realistic low-dimensional semiconductor quantum-wire system. The interacting electrons in the wire are subjected to a linearly polarized time-periodic field. The system is described in atomic units by the Hamiltonian

$$H = \frac{1}{2m^*}p^2 + V(\mathbf{r}) + \lambda \sum_{i>j} \frac{1}{|\mathbf{r}_i - \mathbf{r}_j|} + \beta[\sigma_x p_x (p_y^2 - p_z^2) + \text{cycl.perm.}] + V_0 x \cos(\omega t), \quad (8)$$

where the first three terms represent the kinetic, static-potential, and interelectron Coulomb-potential energies, respectively. The last term is the time-periodic dipole field and the remaining terms represents the Dresselhaus spin-orbit interaction (SOI) due to the bulk inversion asymmetry of the crystal. We find the static solution to the interacting-electron problem in the Hartree-Fock (HF) approximation. By expanding the single-particle spin orbitals in the Bloch form

$$\Phi^0_{qk} = \frac{e^{ikz}}{\sqrt{L}} \sum_{n\sigma} c^{qk}_{n\sigma} \varphi_n(x,y)|\sigma\rangle = \frac{e^{ikz}}{\sqrt{L}} \sum_{n\sigma} c^{qk}_{n\sigma} |n\sigma\rangle, \quad (9)$$

where L is the length of the wire; the HF equation can be cast into the coupled linear system

$$\sum_{n\sigma}\langle m\sigma'|\Big\{\frac{1}{2m^*}(p_x^2+p_y^2+k^2)+V(x,y)+V_H(x,y)+\beta[\sigma_x p_x(p_y^2-p_z^2)+\text{cycl.perm.}]\Big\}|n\sigma\rangle c_{n\sigma}^{qk}+\sum_{q'k',n}\langle m|V_F^{q,k;q'k'}(x,y)|n\rangle c_{n\sigma'}^{q'k'}=E_{qk}^0 c_{m\sigma'}^{qk}, \quad (10)$$

where[18]

$$V_H(x,y)=-\frac{2\lambda}{L}\sum_{qk,mn\sigma} f_{qk}^{\mathrm{FD}}(c_{m\sigma}^{qk})^* c_{n\sigma}^{qk}\times\langle m|\ln(|\boldsymbol{x}-\boldsymbol{x}'|)|n\rangle, \quad (11)$$

and[19]

$$V_F^{q,k;q'k'}(x,y)=-\frac{2\lambda}{L}f_{q'k'}^{\mathrm{FD}}\sum_{m,n\sigma}(c_{m\sigma}^{q'k'})^* c_{n\sigma}^{qk}\times\langle m|K_0(|k-k'||\boldsymbol{x}-\boldsymbol{x}'|)|n\rangle, \quad (12)$$

with $K_0(x)$ being the zeroth-order-modified Bessel function of the second kind. For an efficient numerical method to calculate the HF matrix elements on the form $\langle m'|\langle n'|f(|\boldsymbol{x}-\boldsymbol{x}'|)|n\rangle|m\rangle$, see the Appendix. We note that these equations include fully the SOI and account for the fact that spin is no longer a good quantum number in this system. We solve the HF equations self-consistently through numerical diagonalization in order to find the quasiparticle states Φ_{qk}^0 and energy spectrum E_{qk}^0. By expanding the time-dependent eigensolutions as

$$\Psi_\alpha(\boldsymbol{r},t)=e^{-i\epsilon_\alpha t}\sum_{lq}a_{lq}^\alpha e^{-il\omega t}\Phi_{qk}^0(\boldsymbol{r}), \quad (13)$$

the Hamiltonian, Eq. (8), can be cast into a matrix representation, and diagonalized to yield the set of Hartree-Fock-Floquet eigenstates and the corresponding quasienergy spectrum, in the presence of the time-periodic field. For the numerical solution we scale lengths by the wire width W, energies by $E_0=\pi^2/2m^*W^2$, and fix the parameters $\lambda/WE_0=10\beta/W^3E_0=0.03$ suitable for an InSb wire of width $W=10$ nm. We furthermore set the chemical potential $\mu=5\ E_0$, the time-periodic dipole field strength $V_0W/E_0=0.1$, and consider the arbitrary point $k=1\ \mathrm{W}^{-1}$ at zero temperature.

Figures 3(a) and 3(b) show the calculated HF quasienergy spectrum with the zero-photon and single-photon harmonics $l=\{-1,0,1\}$. In the low-frequency region the states are well separated and show linear dependences on frequency corresponding to $l=\{-1,0,1\}$. Here the geometrical phases of the states are $\chi=\{2\pi,0,-2\pi\}$ indicating a vanishing traced-out circuit in the projective Hilbert space. At $\omega\approx 3\ E_0$ the $l=1$ harmonic dressed states derived from the excited-state anticrosses with the zero-photon ground state. Similarly the $l=-1$ harmonic dressed state derived from the ground state anticrosses with the zero-photon excited state. Without the dipole field the system at nonzero wave vector has the symmetry group C_{2v}, which has only a single two-dimensional double-group representation Γ_5 (Ref. 20). This implies that

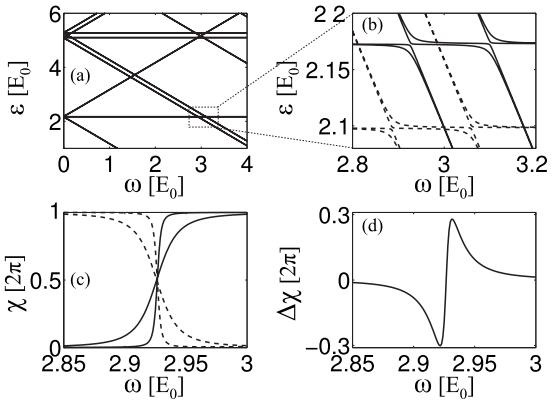

FIG. 3. Numerical Hartree-Fock-Floquet solutions for an InSb nanowire of width $W=10$ nm, described by the Hamiltonian given in Eq. (8) with $\lambda/WE_0=10\beta/W^3E_0=0.03$, $V_0W/E_0=0.1$, chemical potential $\mu=5\ E_0$, and $k=1\ \mathrm{W}^{-1}$. (a) Quasienergy spectrum. (b) Fine scale view of anticrossings. Dashed lines showing a calculation excluding electron-electron interactions for comparison. (c) Geometrical phase of upper (dashed line) and lower (solid line) branches at frequencies around the anticrossing point. (d) Geometric-phase difference around the anticrossing point.

every band is doubly degenerate at all k. The dipole field reduces the symmetry group to C_s, which has two one-dimensional representations Γ_3 and Γ_4, and therefore lifts the degeneracy. Figure 3(b) shows that this degeneracy lifting is most pronounced at anticrossing points where the effect of the hybridizing field is most significant. Since the Hamiltonian $\mathcal{H}$ does not possess time-reversal symmetry there is no additional degeneracy. However, by operating on both sides of Eq. (1) with the time-reversal operator $T=-i\sigma_y K$ (with K being the complex conjugation), we have

$$\left[H-i\frac{\partial}{\partial(-t)}\right]T\Phi_{\alpha pk}(t)=\varepsilon_{\alpha p}(k)T\Phi_{\alpha pk}(t), \quad (14)$$

where we use the fact that the quasienergy is a time-independent quantity. For the Hamiltonian in Eq. (8) the generalized-parity operator is $P=\mathcal{T}R_xR_y\sigma_z$, where $R_{x,y}$ is the spatial-reflection operators and $\mathcal{T}: t\to t+\pi$. It is easy to show that we then have $T\Phi_{\alpha,k,p}(t)=\tilde{\Phi}_{\alpha,-k,-p}(-t)$ which is a state that transforms as the reversed parity and of opposite quasimomentum. We hence find that the generalized-parity quasienergy spectrum must obey the symmetry

$$\varepsilon_{\alpha,p=\pm}(k)=\varepsilon_{\alpha,p=\mp}(-k), \quad (15)$$

which is generalization of the familiar Kramers degeneracy where the generalized parity p takes the role of the "spin" quantum number.

The dashed lines in Fig. 3(b) show the calculated quasienergy without the inclusion of electron-electron interactions. It is seen that the dominant effect of the many-body interactions is an overall increase in energy and an increase in the energy separation between the ground and excited states, resulting in a crossing point at a higher frequency. The qualitative features of the crossings are however not affected by

the many-body interactions. For completeness we shall retain the electron-electron interactions in the remainder of the presented calculations.

The anticrossings result in traced-out circuits in the projective Hilbert space with nontrivial curvatures, and thereby the geometrical phases $\chi \neq 0+2\pi m$, $m \in \mathbb{Z}$, as seen in Fig. 3(c). At the crossing frequencies an exact π phase is found in agreement with the analytical predictions in Sec. II B. Furthermore, the lifting of the twofold degeneracy around the anticrossing point is associated with a separation of the geometrical phases of the parity states. The phase difference follows a dip-peak structure going through the anticrossing point [Fig. 3(d)]. We note that this phase separation is directly related to the presence of spin-orbit interaction in the semiconducting crystal structure of the wire and would vanish for $\beta=0$.

B. Transport measurements of the geometric phase

It is interesting to ask how the geometrical phase affects a conductance measurement through the wire. To this end we consider a quantum wire attached to two leads and consider transport through the four channels participating in one of the anticrossings in Fig. 3. The four channels are grouped in two parity groups and there is no scattering between the groups, whereas the channels within a parity group are hybridized by interchannel scattering at the anticrossing. The carriers are injected in the left lead and collected at the right lead. We label the channels 1–4 counting from lowest to highest energy. In principle there are four geometric phase factors involved. However, the phase factors of the same parity are related as $\chi_{1(2)}=-\chi_{4(3)}$ (cf. Sec. II B). From the Feynman path summation the linear-response conductance from left to right lead is then

$$\frac{G(\beta \neq 0)}{e^2/h} = |t_1 e^{i\chi_1} + t_4 e^{-i\chi_1}|^2 + |t_2 e^{i\chi_2} + t_3 e^{-i\chi_2}|^2$$
$$= \sum_{\alpha=1}^{4} |t_\alpha|^2 + 2\,\mathrm{Re}(t_1 t_4^* e^{i2\chi_1}) + 2\,\mathrm{Re}(t_2 t_3^* e^{i2\chi_2}), \tag{16}$$

where t_α are the complex transmission coefficients from the left to the right lead through channel α.

We may now ask what the result would be if there were no SOI present. We then naturally have $\chi_1=\chi_2$. But now the two anticrossings in Fig. 3(b) collapse into a single anticrossing (cf. inset of Fig. 4) since the first excited state is fourfold degenerate at $V_0=0$ when $\beta=0$. The conductance then takes the form

$$\frac{G(\beta=0)}{e^2/h} = |t_1 e^{i\chi_1} + t_3 + t_5 e^{-i\chi_1}|^2 + |t_2 e^{i\chi_1} + t_4 + t_6 e^{-i\chi_1}|^2. \tag{17}$$

The conductance is in this case modulated by a single geometrical phase which is a result of the phase locking of the interfering channels. Neglecting backscattering we can take the transmission coefficients of the wire of length L to be $t_\alpha=\exp(ikL)/\sqrt{3}$, $\forall \alpha$, with the assumption that transport is taken place at a fixed k number, suitable for a small energy splitting. The conductance then reduces to

$$G(\beta=0) = \frac{2e^2}{h}\frac{1}{3}|1+2\cos(\chi_1)|^2. \tag{18}$$

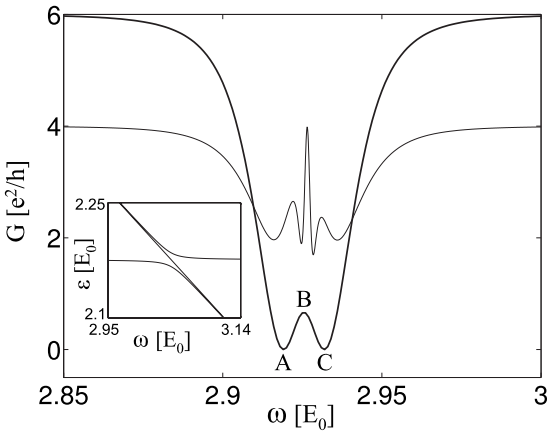

FIG. 4. Conductance through the quantum wire as a function of the frequency of the irradiating field close to the anticrossing point. Thin line with spin-orbit interaction [Eq. (16)] and thick line (shifted by 0.12 E_0 along the ω axis) without spin-orbit interaction [Eq. (18)]. (thick line) At point A the phase-locked states rotate on opposite hemispheres of the Bloch-Riemann sphere with the geometrical phases $\chi=\pm 2\pi/3$. At point B the phase-locked states are rotating on the equator of the sphere, and consequently have a geometrical phases $\chi=\pm\pi$. At point C the states are again rotating on opposite hemispheres with geometrical phases $\chi=\pm 4\pi/3$. The inset shows the quasienergy band anticrossing without SOI.

This is a remarkable result that suggests that the absolute geometrical phase can be measured through the conductance around the anticrossing point. In particular, the extreme points in the conductance are given by $\chi_1=m\pi$, $m2\pi/3 \bmod 2\pi$.

Taking the phases from the numerical solutions the resulting conductance through the wire as a function of the field frequency close to the anticrossing point is shown in Fig. 4. It is seen that the conductance with SOI (thin line) and without SOI (thick line) both share the same general structure. We consider first the non-SOI data. At point A the two phase-locked states are rotating on opposite hemispheres of the Bloch-Riemann sphere with the geometrical phases $\chi=\pm 2\pi/3$ and are destructively interfering with the zero-phase state. The complete cancellation results in zero conductance. At point B the phase-locked states are both rotating on the equator of the sphere with the geometrical phases $\chi=\pm\pi$. The two phase-locked states are hence constructively interfering but are partially cancelled by the zero-phase channel. At point C the same phase situation as in point A again occurs except the states have now switched hemispheres in relation to point A. For the case of nonvanishing SOI there are only two phase-locked interfering channels. The lifting of the two geometrical phases means that there is now no complete cancellation at points A and C. Furthermore, at point B all states are rotating on the equator of the sphere and hence

$\chi_1=\chi_2$. This leads to a complete constructive interference resulting in full conductance.

The phase evolution through the crossing point results in distinct conductance features which enables the identification of the geometrical phase. Although the phase at points A and C are dependent on the ratio of the channel transmission coefficients, and thus the coupling of the channels to the leads, the π phase at point B does not depend on this ratio and can hence be uniquely identified from the central conductance extreme point.

IV. CONCLUSION

A time-periodic field with photon energy of the order of the level separation opens up dynamical anticrossings in the photon-dressed-state spectrum of a quantum system. At photon energies of the driving field close to these anticrossing points, circuits traced out by the eigenstates in the projective Hilbert space show a nontrivial topology. The induced geometrical phase is directly related to the Rabi frequency in the transition between the anticrossing states.

We have examined, by exploiting the Floquet theory, an interacting-electron spin-orbit-coupled nanowire system under the influence of a time-periodic field. We have illustrated the generic properties of the geometrical phase with dynamic responses of the quasienergy spectra found by numerical diagonalization. The anticrossing states exhibit a phase locking between equal parity states and the phase separation between opposite parity states is spin-orbit interaction dependent. The interference of conductance channels in a quantum wire presents a way to identify the geometrical-phase evolution close to anticrossing points in the quasienergy spectrum.

APPENDIX

Alavi showed in Ref. 21 how the Coulomb integral can be expanded in a Fourier series in a cuboidal geometry. For completeness we here repeat the procedure for the Hartree and Fock matrix elements.

We can expand the function $f(|\boldsymbol{x}-\boldsymbol{x}'|)$ in a discrete Fourier series

$$f(|\boldsymbol{x}-\boldsymbol{x}'|)=\sum_{\boldsymbol{g}} v_{\boldsymbol{g}} e^{i\pi \boldsymbol{g}\cdot(\boldsymbol{x}-\boldsymbol{x}')}, \tag{A1}$$

with $\boldsymbol{g}\in\mathbb{Z}^3$ and the coefficients

$$v_{\boldsymbol{g}}=\frac{1}{\Omega}\int_{\Omega} d\boldsymbol{x} e^{-i\boldsymbol{g}\cdot\boldsymbol{x}} f(|\boldsymbol{x}-\boldsymbol{x}'|). \tag{A2}$$

Here the domain of integration is the maximum displacement in the wire cross section $x,y\in[-1,1]$, implying $\Omega=4$. The two-body matrix element integrals occurring in Eqs. (10)–(12) can then be cast into a sum of products

$$\langle m'|\langle n'|f(|\boldsymbol{x}-\boldsymbol{x}'|)|n\rangle|m\rangle = \sum_{\boldsymbol{g}} v_{\boldsymbol{g}} (I_{g_x n'_x n_x} I_{g_y n'_y n_y} I_{-g_x m'_x m_x} I_{-g_y m'_y m_y}), \tag{A3}$$

where $I_{gn'_x n_x}=\langle n'_x|\exp(ig\pi x)|n_x\rangle$. Taking $|n_x\rangle=\sqrt{2}\sin(n_x\pi x)$ we have

$$I_{gn'_x n_x}=\frac{1}{2}(I^0_{n_x-m_x+g_x}+I^0_{-n_x+m_x+g_x}-I^0_{n_x+m_x+g_x}-I^0_{-n_x-m_x+g_x}), \tag{A4}$$

where

$$I^0_k=\int_0^1 dx e^{ik\pi x}=\begin{cases}\dfrac{(-1)^k-1}{ik\pi}, & k\neq 0\\ 1, & k=0\end{cases}. \tag{A5}$$

*brusheimp@ihpc.a-star.edu.sg
†hongqi.xu@ftf.lth.se

[1] M. V. Berry, Proc. R. Soc. London, Ser. A **392**, 45 (1984).
[2] B. Simon, Phys. Rev. Lett. **51**, 2167 (1983).
[3] Y. Aharonov and J. Anandan, Phys. Rev. Lett. **58**, 1593 (1987).
[4] J. Anandan and Y. Aharonov, Phys. Rev. D **38**, 1863 (1988).
[5] J. Samuel and R. Bhandari, Phys. Rev. Lett. **60**, 2339 (1988).
[6] D. Suter, K. T. Mueller, and A. Pines, Phys. Rev. Lett. **60**, 1218 (1988).
[7] Y. Zhang, Y.-W. Tan, H. L. Stormer, and P. Kim, Nature (London) **438**, 201 (2005).
[8] K. S. Novoselov, E. McCann, S. V. Morozov, V. I. Fal'ko, M. I. Katsnelson, U. Zeitler, D. Jiang, F. Schedin, and A. K. Geim, Nat. Phys. **2**, 177 (2006).
[9] M. Möttönen, J. J. Vartiainen, and J. P. Pekola, Phys. Rev. Lett. **100**, 177201 (2008).
[10] N. Kang, K. Suzuki, E. Abe, Y. Hashimoto, Y. Iye, and S. Katsumoto, Physica E (Amsterdam) **40**, 1051 (2008).
[11] R. Capozza, D. Giuliano, P. Lucignano, and A. Tagliacozzo, Phys. Rev. Lett. **95**, 226803 (2005).
[12] P. J. Leek, J. M. Fink, A. Blais, R. Bianchetti, M. Göppl, J. M. Gambetta, D. I. Schuster, L. Frunzio, R. J. Schoelkopf, and A. Wallraff, Science **318**, 1889 (2007).
[13] E. Sjöqvist, Physics **1**, 35 (2008).
[14] D. J. Moore, J. Phys. A **23**, L665 (1990).
[15] A. Mostafazadeh, J. Phys. A **31**, 9975 (1998).
[16] M. Grifoni and P. Hänggi, Phys. Rep. **304**, 229 (1998).
[17] C. M. Wilson, T. Duty, F. Persson, M. Sandberg, G. Johansson, and P. Delsing, Phys. Rev. Lett. **98**, 257003 (2007).
[18] A. Brataas, V. Gudmundsson, A. G. Mal'shukov, and K. A. Chao, J. Phys.: Condens. Matter **10**, 4267 (1998).
[19] S. Ihnatsenka and I. V. Zozoulenko, J. Phys.: Condens. Matter **20**, 335233 (2008).
[20] G. F. Koster, J. O. Dimmock, R. G. Wheeler, and Hermann Statz, *Properties of the Thirty-Two Point Groups* (MIT, Cambridge, 1963).
[21] A. Alavi, J. Chem. Phys. **113**, 7735 (2000).